Robust reduced-order controller of laminar boundary layer transitions

L. Cortelezzi and J. L. Speyer
Department of Mechanical and Aerospace Engineering, University of California, Los Angeles, California 90095-1597
(Received 2 February 1998)

A framework to derive optimal and robust reduced-order controllers of fluid mechanics and plasma physics flows using linear-quadratic-Gaussian design, or, in modern terms, $\mathcal{H}_2$ design, is presented. As a test case, two-dimensional channel flow is considered. A reduced model is derived, and a controller is designed based upon this model. Initial conditions creating transient growth of wall-shear stress are constructed. The controller is tested on a 32 wave number simulation. A wall-shear stress reduction, up to 90%, is obtained. The potential transferability of the controller to engineering applications is discussed. [S1063-651X(98)06408-8]

PACS number(s): 47.62.+q, 47.27.Cn, 47.27.Rc, 47.27.Vf

The reduction of drag produced by skin friction, or, in other words, the reduction of wall-shear stresses (WSS's) generated by near-wall turbulence have received wide attention. ''The skin friction constitutes about 50%, 90%, and 100% of the total drag on commercial aircraft, underwater vehicles, and pipelines, respectively'' [1]. Two are the near-wall flows of interest: boundary layers that change from laminar to turbulent regimes, and boundary layers that are inherently turbulent. Correspondingly, efforts to reduce skin friction fall into two broad categories: transition inhibition and turbulence suppression. References [1–4] are recent reviews summarizing achievements and open questions in boundary layer control.

Boundary layer control has been attempted with some success. References [5–23] are articles published in the past four years. It is becoming widely accepted that even better results can be obtained by using controllers able to analyze distributed measurements and coordinate distributed actuators. However, very little has been done [24–26] to exploit the tools recently developed in the control community [27,28]. In particular, linear-quadratic-Gaussian (LQG) design, or, in modern terms, $\mathcal{H}_2$ design, combined with model reduction techniques for multiinput-multioutput (MIMO) systems, has never been used in fluid mechanics nor plasma physics.

Using a case study, this paper introduces the reader to a framework for deriving optimal and robust reduced-order controllers for flows of interest in fluid mechanics and plasma physics. As a case study, we show that MIMO LQG ($\mathcal{H}_2$) design can be successfully applied to suppress up to 90% of the WSS in a two-dimensional transitional channel flow. The framework can be easily applied to control problems described over simple domains (rectangles, circles and ellipsis, cubes, cylinders, tori, etc.) by linear partial differential equations with nonhomogeneous boundary conditions. The spectral decomposition depends on the geometry of the problem and, consequently, appropriate base functions should be selected. Once the spectral decomposition is in order, the framework can be applied step by step. In the case when there is more than one partial differential equation, the state space equations for the full problem are obtained by stacking the ordinary differential equations generated by the Galerkin projection of each partial differential equation. This paper also addresses the potential transferability of the controller to engineering applications.

We consider two-dimensional incompressible Poiseuille flow in a periodic channel of length Lh and height $2h$. The undisturbed velocity field has a parabolic profile with centerline velocity U_c: see Fig. 1. Since we are interested in controlling the transition of the boundary layer from laminar to turbulent regimes, we consider a small perturbation of flow quantities. The reader should be aware that with the term ''transition,'' we identify the disruption of the laminar regime in a fully developed boundary layer due to the growth of spatially localized near-wall perturbations. The linearized Navier-Stokes equations are written in terms of the perturbation stream-function ψ,

$$(\partial_t + U\partial_x)\triangle\psi - U''\psi_x = \mathrm{Re}^{-1}\triangle\triangle\psi, \tag{1}$$

to satisfy continuity identically. The problem is made dimensionless by using h as a characteristic length and h/U_c as a characteristic time. The Reynolds number is $\mathrm{Re}=U_c h/\nu$.

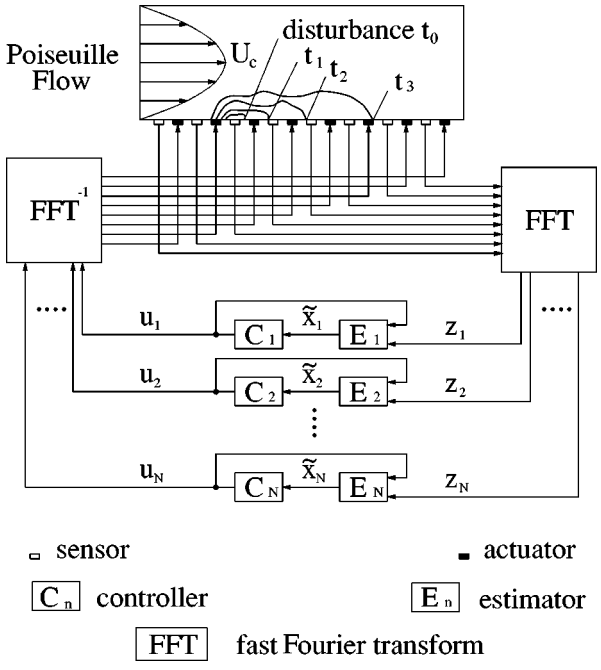

FIG. 1. Controller architecture.

To suppress perturbations evolving within the bottom boundary layer, we apply blowing and suction at the bottom wall (see Fig. 1). For simplicity we assume that the actuators are uniformly distributed. Perturbations in the top boundary layer are left free to evolve. The corresponding boundary conditions are

$$\psi_x|_{y=-1} = -v_w(x,t), \quad \psi_y|_{y=\pm 1} = \psi|_{y=1} = 0, \tag{2}$$

where the control function v_w prescribes the amount of blowing and suction at the bottom wall. We impose that the mass of fluid injected equals the mass of fluid removed.

To detect and measure the deviations of the boundary layer from the laminar regime, we measure the gradient of the streamwise velocity component at given points $x = x_i$ along the bottom wall (see Fig. 1),

$$z(x_i,t) = \psi_{yy}|_{y=-1}. \tag{3}$$

In other words, we measure the first term of the WSS, $\tau_{yx} = \mathrm{Re}^{-1}(\psi_{yy} - \psi_{xx})|_{y=-1}$. The second term of the WSS is zero in the uncontrolled case, and is known in the controlled case.

We define an optimal performance index J, or cost function, to design a controller for the LQG ($\mathcal{H}_2$) problem. Since we are interested in suppressing the WSS, we define

$$J = \lim_{t_f \to \infty} \int_t^{t_f} \int_0^L (\psi_{yy}^2 + \psi_{xx}^2)|_{y=-1} dx\, dt. \tag{4}$$

The integrand represents the cost of the WSS being different from zero. Moreover, the integrand implicitly accounts for the cost of implementing the control itself. There are two reasons to minimize the cost of the controller: In any engineering application the energy available to drive the controller is limited, and a large control action may drive the system away from the region where the linear model is valid.

To reduce Eqs. (1)–(3) to a set of first-order ordinary differential equations, we make a few transformations loosely based on Refs. [24] and [26]. We write the stream function as $\psi = \phi + \chi$ to embed the actuator into the evolution equation, and to make the boundary conditions homogeneous. Substituting $\psi = \phi + \chi$ into Eq. (1), we obtain a forced equation for the Poiseuille flow

$$\begin{aligned}(\partial_t + U\partial_x)\triangle\phi - U''\phi_x &= \mathrm{Re}^{-1}\triangle\triangle\phi \\ &\quad - (\partial_t + U\partial_x)\triangle\chi + U''\chi_x \\ &\quad + \mathrm{Re}^{-1}\triangle\triangle\chi,\end{aligned} \tag{5}$$

with homogeneous boundary conditions $\phi|_{y=\pm 1} = \phi_y|_{y=\pm 1} = 0$. The forcing function χ satisfies the nonhomogeneous boundary conditions (2), i.e., $\chi_x|_{y=-1} = -v_w(x,t)$, $\chi|_{y=1} = \chi_y|_{y=\pm 1} = 0$. We also substitute $\psi = \phi + \chi$ into Eqs. (3) and (4). The measurement equation (3) becomes

$$z(x_i,t) = (\phi_{yy} + \chi_{yy})|_{x=x_i, y=-1}, \tag{6}$$

while the cost function (4) takes the following form:

$$J = \lim_{t_f \to \infty} \int_t^{t_f} \int_0^L [(\phi_{yy} + \chi_{yy})^2 + \chi_{xx}^2]_{y=-1} dx\, dt. \tag{7}$$

Subsequently, flow quantities are spectrally decomposed by using circular functions in the streamwise direction and Chebyshev polynomials in the vertical direction. We expand ϕ and χ as follows:

$$\phi = \sum_{n=1}^{N} \sum_{m=0}^{M} [a_{nm}(t)\cos(\alpha_n x) + b_{nm}(t)\sin(\alpha_n x)] C_m(y), \tag{8}$$

$$\chi = \sum_{n=1}^{N} [p_n(t)\cos(\alpha_n x) + q_n(t)\sin(\alpha_n x)] D(y), \tag{9}$$

where $\alpha_n = 2\pi n/L$. Functions C_m and D are combinations of Chebyshev polynomials constructed to satisfy the boundary conditions, i.e., $C_m(\pm 1) = C_m'(\pm 1) = D(1) = D'(\pm 1) = 0$ and $D(-1) = 1$. We also expand the measurement function z as follows:

$$z = \sum_{n=1}^{N} [c_n(t)\cos(\alpha_n x) + d_n(t)\sin(\alpha_n x)]. \tag{10}$$

Substituting expansions (8), (9), and (10) into equations (5) and (6) and using Galerkin's projection, we obtain

$$\frac{d\boldsymbol{y}}{dt} = \boldsymbol{A}\boldsymbol{y} + \boldsymbol{B}_1\boldsymbol{u} + \boldsymbol{B}_2\frac{d\boldsymbol{u}}{dt}, \quad \boldsymbol{z} = \boldsymbol{C}\boldsymbol{y} + \boldsymbol{D}_3\boldsymbol{u}. \tag{11}$$

To transform the above equations into standard state-space form, we define a new vector $\boldsymbol{x} = \boldsymbol{y} + \boldsymbol{B}_2\boldsymbol{u}$, and two new matrices $\boldsymbol{B} = \boldsymbol{B}_1 + \boldsymbol{A}\boldsymbol{B}_2, \boldsymbol{D} = \boldsymbol{D}_3 + \boldsymbol{C}\boldsymbol{B}_2$. Finally, we obtain the state-space equations

$$\frac{d\boldsymbol{x}}{dt} = \boldsymbol{A}\boldsymbol{x} + \boldsymbol{B}\boldsymbol{u}, \quad \boldsymbol{z} = \boldsymbol{C}\boldsymbol{x} + \boldsymbol{D}\boldsymbol{u}, \tag{12}$$

with initial condition $\boldsymbol{x}(0) = \boldsymbol{x}_0$, where $\boldsymbol{x}$ is the internal state vector, $\boldsymbol{u}$ is the control vector, and $\boldsymbol{z}$ is the measurement vector. Matrices $\boldsymbol{A}$, $\boldsymbol{B}$, and $\boldsymbol{C}$ contain the dynamics of the Poiseuille flow, actuators, and sensors, respectively. Matrix $\boldsymbol{D}$ contains the direct coupling between sensors and actuators. The cost function (7) becomes

$$J = \lim_{t_f \to \infty} \int_t^{t_f} [\boldsymbol{z}^T\boldsymbol{z} + \boldsymbol{u}^T\boldsymbol{W}^T\boldsymbol{W}\boldsymbol{u}] dt, \tag{13}$$

where the superscript ^{T} denotes transpose. The matrix $\boldsymbol{W}$ is obtained by spectrally decomposing the last term in the cost function (7).

The advantage of the present formulation is that the whole problem decouples with respect to the wave number. All matrices in Eqs. (12) and (13) are block diagonal. The block diagonal structure of the matrix $\boldsymbol{A}$ was first recognized in Ref. [24]. The above state-space system is consequently equivalent to N state-space subsystems, one for each wave number. For a given wave number r the state-space equations are

$$\frac{d\boldsymbol{x}_r}{dt} = \boldsymbol{A}_r\boldsymbol{x}_r + \boldsymbol{B}_r\boldsymbol{u}_r, \quad \boldsymbol{z}_r = \boldsymbol{C}_r\boldsymbol{x}_r + \boldsymbol{D}_r\boldsymbol{u}_r, \tag{14}$$

with initial condition $\boldsymbol{x}_r(0)=\boldsymbol{x}_{r0}$. Vectors $\boldsymbol{x}_r$, $\boldsymbol{u}_r$, and $\boldsymbol{z}_r$ have the following structure: $\boldsymbol{x}_r=[a_{r0},\ldots,a_{rM},b_{r0},\ldots,b_{rM}]^T$, $\boldsymbol{u}_r=[p_r,q_r]^T$, $\boldsymbol{z}_r=[c_r,d_r]^T$. The cost function also decouples with respect to the wave number, and we obtain N optimal performance indexes. For a given wave number r, the cost function is defined as follows:

$$J_r=\lim_{t_f\to\infty}\int_t^{t_f}[\boldsymbol{z}_r^T\boldsymbol{z}_r+\boldsymbol{u}_r^T\boldsymbol{W}_r^T\boldsymbol{W}_r\boldsymbol{u}_r]dt. \tag{15}$$

Consequently, the design of an optimal and robust controller for system (12) with Eq. (13) has been reduced to the independent design of N optimal and robust controllers, one for each wave number, for the subsystems (14) with Eq. (15).

The challenge of the present study is to reduce the size of the controller. The controller of the full system would have $2N(M+1)$ states. A controller with thousands of states is of no interest in engineering applications, because of the amount of hardware and computer power necessary to compute a real-time control law. We derive a lower order controller in two steps: First we construct a lower order model of Eq. (14), and subsequently we design an optimal and robust controller for the reduced-order model. To obtain a lower order model, we transform Eq. (14) into Jordan canonical form. The matrices $\hat{\boldsymbol{A}}_r$, $\hat{\boldsymbol{B}}_r$, $\hat{\boldsymbol{C}}_r$, and $\boldsymbol{D}_r$ that describe the dynamics of the reduced-order model are obtained from the matrices in Jordan canonical form by retaining rows and columns corresponding to equally well controllable or observable states. Hat denotes the quantities associated with the reduced-order model.

The design of an optimal and robust controller for the LQG ($\mathcal{H}_2$) problem is divided in two parts: the linear quadratic regulator (LQR) and the minimum variance estimator (Kalman-Bucy filter) [27,28]. The LQR provides an optimal control law in terms of the internal state vector. In general, however, the internal state vector is not directly measurable. The Kalman-Bucy filter provides an optimal estimate of the internal state vector in terms of the measurement vector $\boldsymbol{z}_r$. The result of the LQG ($\mathcal{H}_2$) design of an optimal and robust controller based on the reduced-order model of Eq. (14) is summarized by the following equations:

$$\boldsymbol{u}_r=-\hat{\boldsymbol{K}}_r\tilde{\boldsymbol{x}}_r, \tag{16}$$

$$\frac{d\tilde{\boldsymbol{x}}_r}{dt}=\hat{\boldsymbol{A}}_r\tilde{\boldsymbol{x}}_r+\hat{\boldsymbol{B}}_r\boldsymbol{u}_r+\hat{\boldsymbol{L}}_r[\boldsymbol{z}_r-\hat{\boldsymbol{C}}_r\tilde{\boldsymbol{x}}_r-\boldsymbol{D}_r\boldsymbol{u}_r], \tag{17}$$

with initial conditions $\tilde{\boldsymbol{x}}_r(0)=\boldsymbol{0}$. Equation (16) is the control law. The gains matrix $\hat{\boldsymbol{K}}_r$ is obtained by minimizing the optimal performance index

$$\hat{J}_r=\lim_{t_f\to\infty}\int_t^{t_f}[\hat{\boldsymbol{z}}_r^T\hat{\boldsymbol{z}}_r+\boldsymbol{u}_r^T\boldsymbol{W}_r^T\boldsymbol{W}_r\boldsymbol{u}_r]dt, \tag{18}$$

where $\hat{\boldsymbol{z}}_r=\hat{\boldsymbol{C}}_r\hat{\boldsymbol{x}}_r-\boldsymbol{D}_r\boldsymbol{u}_r$. Equation (17) is the the minimum variance estimator. The matrix $\hat{\boldsymbol{L}}_r$ is obtained by minimizing the variance of the estimated state vector $\tilde{\boldsymbol{x}}_r$ with respect to the internal state vector $\hat{\boldsymbol{x}}_r$ assuming that the reduced model of Eq. (14) is affected by additive Gaussian white noise. In this study, however, the power spectral densities of the additive noise are used as design parameters to produce robust controllers. The initial condition $\tilde{\boldsymbol{x}}_r(0)=\boldsymbol{0}$ implies that the estimator starts with no information about $\hat{\boldsymbol{x}}_r$.

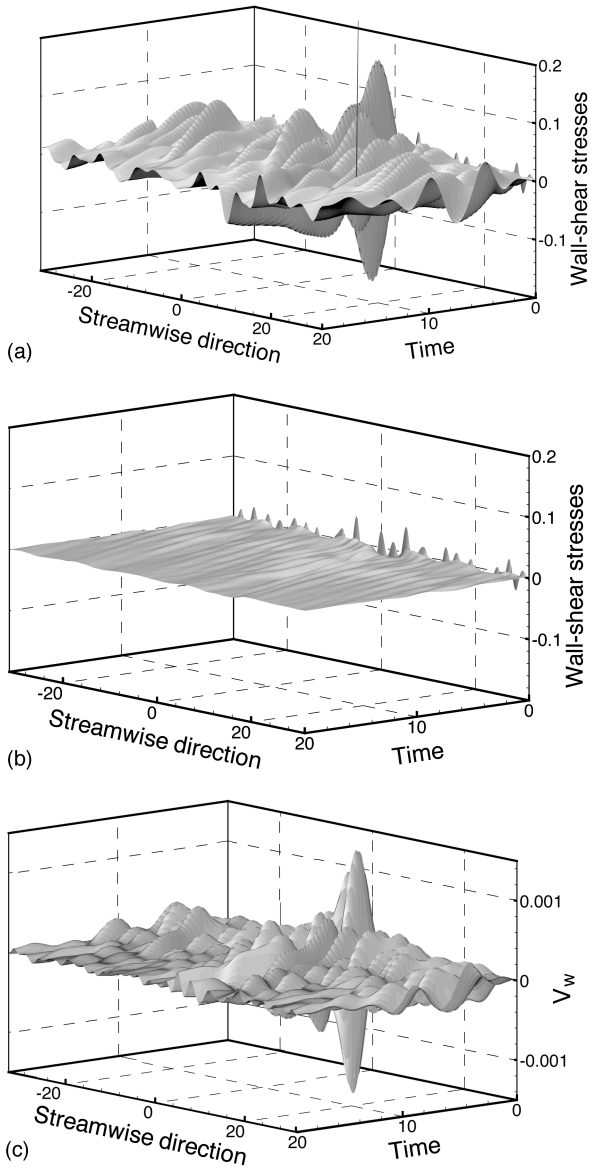

FIG. 2. Temporal evolution of wall-shear stress along the bottom wall of the channel: uncontrolled case (a); controlled case (b). Temporal evolution of blowing and suction along the bottom wall of the channel (c).

Figure 1 links with simplicity the mathematical formulation to its computational implementation, by summarizing in a block diagram the control strategy described above. The controller can be programmed in a computer routine whose input is an array containing the gradients of the streamwise velocity component, and whose output is an array containing the blowing and suction at the wall. The gradient of the streamwise velocity component, ψ_{yy}, is converted by a fast Fourier transform (FFT) into $\boldsymbol{z}_r$'s. Each pair of estimator (17) and controller (16) blocks is integrated in time by, for example, a third-order low-storage Runge-Kutta scheme. Parallel computation produces $\boldsymbol{u}_r$'s. An inverse FFT converts $\boldsymbol{u}_r$'s into the actuating signal v_w. This routine can be embed-

ded in any Navier-Stokes solver able to handle time-dependent boundary conditions for the control of more realistic two-dimensional transitional boundary layers [29].

Figure 1 also provides the basic architecture for the potential implementation of the present controller in practical engineering applications. The gradient of the streamwise velocity component, ψ_{yy}, can be measured by microelectromechanical-systems (MEMS) hot film sensors [30]. Analog to digital converters (A/D) and digital signal processors (DSP's) convert the measured gradients into $\mathbf{z}_r$'s. Each pair of estimator (17) and control (16) blocks is replaced by a microprocessor, and a parallel computation produces $\boldsymbol{u}_r$'s. A DSP and a digital to analog converter (D/A) produce the actuating signal. Finally, MEMS technology will provide the necessary hardware. Note that a variety of actuators can mimic small amplitude blowing and suction at the wall: porous walls, micropumps, deformable walls, and thermal actuators [30].

We use a combination of unsteady modes and transient growth to create a worse scenario test case. We choose the Reynolds number and channel length in order to have at least a few unstable modes. The nonorthogonality of the eigenfunctions associated with Eq. (1) permits us to construct initial conditions leading to transient growth; see Ref. [3] for references. We obtain initial conditions specifically able to generate transient growth of the WSS, instead of internal energy, by modifying a technique proposed in Ref. [31]. Although transient growth will be eventually subdued by the viscous effects, it permits testing the capability of the controller in suppressing disturbances that can trigger nonlinear effect and transition to turbulence.

We design a controller for two-dimensional Poiseuille flow in a periodic channel of length $L=20\pi$ at $\mathrm{Re}=10\,000$. The wave numbers $n=8,9$, and 10 are unstable. We use a grid resolution of $N=32$ and $M=124$. The order of the full system is 8000. Using the model reduction technique previously described, we create a reduced model of order 640. This reduced model maximizes the ratio between performance and the number of states. We derive 32 controllers of order 20, one for each wave number. Controllers operate in parallel. Figure 2(a) shows the temporal evolution of the WSS along the bottom wall of the channel for the uncontrolled case. The WSS presents a rich structure because of the transient growth of 32 stable and unstable wave numbers. Figures 2(b) and 2(c) show the temporal evolution of the controlled WSS and of the blowing and suction along the bottom wall of the channel. Although the estimator starts with no information about the internal state of the system, the controller reduces the initial WSS in the first few time steps. Subsequently, the amplitude of blowing and suction rises to suppress the effects of transient growth. Eventually, blowing and suction decreases as the transient growth subdues. The controlled WSS shows only some low amplitude ripples during the entire simulation. The comparison of the Figs. 2(a) and 2(b) shows up to 90% WSS reduction. The remaining unsuppressed WSS is due to the modes that cannot be controlled. The performance of the controller can be improved at the price of increasing its order.

In conclusion, we presented a framework for the application of LQG ($\mathcal{H}_2$) design and model reduction to flows of interest in fluid mechanics and plasma physics. As a case study, this framework has been used to design an optimal and robust reduced-order controller able to suppress up to 90% of the WSS in a two-dimensional transitional channel flow. This controller can be programmed in a computer routine whose inputs are the gradients of the streamwise velocity component, and whose outputs are the blowing and suction at the wall. This routine, suited for parallel computing, can be embedded in any Navier-Stokes solver for the control of more realistic two-dimensional transitional boundary layers [29]. We also presented a hardware architecture for the potential implementation of the controller in engineering applications. Extensions of LQG ($\mathcal{H}_2$) design and applications of $\mathcal{H}_\infty$ design [27,28] to three-dimensional Poiseuille flow and two- and three-dimensional Blasius boundary layers are in progress.

The authors thank Dr. J. Burns, Dr. S. Joshi, Dr. R.E. Kelly, Dr. J. Kim, and Dr. R.T. MCloskey for enlightening discussions. This work was supported by AFOSR Grant No. F49620-97-1-0276 and by NASA Grant No. NCC 2-374 Pr 41.

[1] M. Gad-el-Hak, AIAA J. **32**, 1753 (1994).
[2] V. J. Modi, J. Fluids Struct. **11**, 627 (1997).
[3] H. L. Reed, W. S. Saric, and D. Arnal, Annu. Rev. Fluid Mech. **28**, 389 (1996).
[4] R. W. Barnwell and M. Y. Hussaini *Natural Laminar Flow and Laminar Flow Control* (Springer-Verlag, New York, 1992).
[5] P. Koumoutsakos, Phys. Fluids **9**, 3808 (1997).
[6] R. Rathnasingham and K. S. Breuer, Phys. Fluids **9**, 1867 (1997).
[7] C. Lee, J. Kim, D. Babcock, and R. Goodman, Phys. Fluids **9**, 1740 (1997).
[8] C. H. Crawford and G. E. Karniadakis, Phys. Fluids **9**, 788 (1997).
[9] T. Kato, Y. Fukunishi, and R. Kobayashi, JSME Int. J. Ser. B Fluids Thermal Eng. **40**, 536 (1997).
[10] P. A. Nelson, M. C. M. Wright, and J. L. Rioual, AIAA J. **35**, 85 (1997).
[11] H. A. Carlson and J. L. Lumley, J. Fluid Mech. **329**, 341 (1996).
[12] B. F. Farrell and P. J. Ioannou, Phys. Fluids **8**, 1257 (1996).
[13] R. D. Joslin, G. Eriebacher, and M. V. Hussaini, J. Fluids Eng. Trans. ASME **118**, 494 (1996).
[14] T. Lee, M. Fisher, and W. H. Schwarz, J. Fluid Mech. **288**, 37 (1995).
[15] P. Hackenberg, J. L. Rioual, O. R. Tutty, and P. A. Nelson, Appl. Sci. Res. **54**, 293 (1995).
[16] U. Rist and H. Fasel, J. Fluid Mech. **298**, 211 (1995).
[17] S. Hubbard and N. Riley, Int. J. Heat Mass Transf. **38**, 3209 (1995).

[18] R. D. Joslin *et al.*, AIAA J. **33**, 1521 (1995).
[19] H. H. Hu and H. H. Bau, Proc. R. Soc. London, Ser. A **447**, 299 (1994).
[20] J. Jimenez, Phys. Fluids **6**, 944 (1994).
[21] M. M. Elrefaee, Eng. Anal. Boundary Elements **14**, 239 (1994).
[22] A. H. M. Kwong and A. P. Dowling, AIAA J. **32**, 2409 (1994).
[23] H. Choi, P. Moin, and J. Kim, J. Fluid Mech. **262**, 75 (1994).
[24] S. S. Joshi, J. L. Speyer, and J. Kim, J. Fluid Mech. **332**, 157 (1997).
[25] S. N. Singh and P. R. Bandyopadhyay, J. Fluids Eng. Trans. ASME **119**, 852 (1997).
[26] S. S. Joshi, J. L. Speyer, and J. Kim, *Proceedings of the 34th IEEE Conference on Decision and Control, New Orleans, LA, December 1995* (IEEE, New York, 1995), p. 921.
[27] K. Zhou, J. C. Doyle, and K. Glover, *Robust and Optimal Control* (Prentice Hall, Englewood Cliffs, NJ, 1996).
[28] I. Rhee and J. L. Speyer, IEEE Trans. Autom. Control. **36**, 1021 (1996).
[29] L. Cortelezzi, K. H. Lee, J. Kim, and J. L. Speyer, Int. J. Comput. Fluid Dyn. (to be published).
[30] C. M. Ho and Y. C. Tai, J. Fluids Eng. Trans. AMSE **118**, 437 (1996).
[31] B. F. Farrell, Phys. Fluids **31**, 2093 (1988).